Analysis of concrete-filled steel tubular columns with "T" shaped cross section (CFTTS)

Qin-Ting Wang and Xu Chang[*]

*College of Civil Engineering; Henan Polytechnic University; Jiaozuo City,
Henan Province, 454000; People's Republic of China*

Abstract.   This paper presents a numerical study of axially loaded concrete-filled steel tubular columns with "T" shaped cross section (CFTTS) based on the ABAQUS standard solver. Two types of columns with "T" shaped cross section, the common concrete-filled steel tubular columns with "T" shaped cross section (CCFTTS) and the double concrete-filled steel tubular columns with "T" shaped cross section (DCFTTS), are discussed. The failure modes, confining effects and load-displacement curves are analyzed. The numerical results indicate that both have the similar failure mode that the steel tubes are only outward buckling on all columns' faces. It is found that DCFTTS columns have higher axial capacities than CCFTTS ones duo to the steel tube of DCFTTS columns can plays more significant confining effect on concrete. A parametric study, including influence of tube thickness, concrete strength and friction coefficient of tube-concrete interface on the axial capacities is also carried out. Simplified formulae were also proposed based on this study.

Keywords: axial capacity; concrete-filled steel tube; T-shaped cross section; confining effect

1. Introduction

Over the last several decades, concrete-filled steel tubular (CFT) structure is widely used in the construction of modern buildings and bridges, even in regions of high seismic risk. This composite construction ideally combines the advantages of both steel tube and concrete, namely the speed of construction and high strength. Moreover, they have lighter weight, higher bending stiffness, and better cyclic performance than the reinforced concrete construction.

Also, significant efforts have been devoted to investigation of the behaviors of concrete filled steel tube columns both in theoretical analyses and tests (Chang *et al.* 2012, Ellobody *et al.* 2006, Han 2007, Han *et al.* 2005a, Nardin and Debs 2007, Shanmugam and Lakshmi 2001, Tao *et al.* 2009, Uenaka *et al.* 2008, Uy 2001). However, most of existing studies focused on concrete-filled tubular columns with circular and square/rectangular cross sections. In recent years, concrete-filled steel tube columns with L-, T-, and +-shaped cross-sections have attracted a significant attention from engineers and architects owing to their aesthetic appearance and structural benefits. The sectional thickness of the special shaped CFT columns can be designed in accordance with the

---

∗Corresponding author, Associate Professor, E-mail: changxu815@163.com

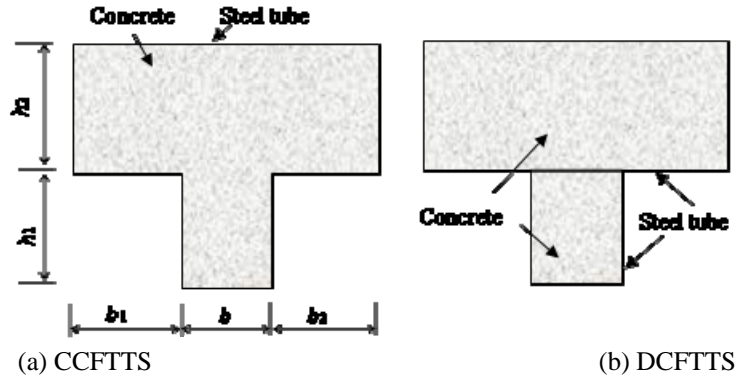(a) CCFTTS   (b) DCFTTS

Fig. 1 Cross sections for special shaped concrete filled steel tube column

thickness of adjacent walls. Compared with CFT columns with circular and square/rectangular cross-sections, they have the advantage of not extending beyond walls, resulting in an enlarged useful indoor area. Despite its increasing use in recent years, only a few papers on the research of concrete-filled steel tube columns with special shaped cross section can be found (Du *et al*. 2008, Xu *et al*. 2009). The lack of research on special shaped CFT columns impaired its broader use in construction.

In this contribution, the behavior of CFTTS columns with two different T-shape cross-sections (as shown in Fig. 1) is discussed here. In physical tests, the steel tube indicated in section (a) is welded by one steel plate (CCFTTS) and the steel tube shown in section (b) is welded by two steel tubes with square/rectangular cross section (DCFTTS). Physical testing is expensive and time consuming, and it is also very difficult to conduct extensive parametric studies by experiments. Thus, encouraging the use and development of numerical modeling in engineering researches is important. The ABAQUS/standard solver is employed to investigate and predict the axial compressive resistances and the failure modes of CFTTS columns in this study. Validation of this numerical method is carried out by comparing the simulation results with the experimental observation of eleven physical tests. A parametric study, including the thickness of steel tube and strengths of concrete, is also carried out. It is expected that the results of this numerical study are beneficial to understand the mechanical behavior and design the CFTTS columns.

2. Description of the numerical modeling method

2.1 Sample preparation

Material properties specified in ABAQUS include a Young's modulus of steel (E_s) of 210 GPa and a Poisson's ratio μ_s of 0.28. The steel is assumed to behave as an elastic-plastic material with isotropic strain hardening in compression. Strain hardening had been modeled based on incremental plasticity theory. A hardening rigidity of 2% E_s after yield has been adopted.

The damaged plasticity model defined in Standard ABAQUS is used in the analysis (Hibbitt, Karlson & Sorensen Inc. 2003). By using the finite element method, strength improvement at the state of triaxial loading can be achieved by the definition of the yielding surface, and the

description of the plastic behavior comes from the equivalent stress-strain relationship of core concrete. Many previous studies indicated that the behaviors of concrete core depended strongly on the passive confinement of the steel tube. Different depth to thickness ratios of rectangular steel tubes provide variable confinement for the concrete, therefore it is an arduous task to describe the uniaxial stress-strain relationship for concrete core of concrete filled rectangular steel tubular columns precisely (ACI 1999, Hu and Schnobrich 1989, Mander *et al*. 1988, Hu *et al*. 2003, Saenz 1964). The widely accepted equivalent stress-strain model proposed by Han *et al*. (2005b) based on a large amount test results is used in this paper. As the model has been fully documented by Han *et al*. (2005b), so we only briefly describes as following

$$y = \begin{cases} 2x - x^2 & (x \leq 1) \\ \dfrac{x}{\beta_0(x-1)^{\eta} + x} & (x > 1) \end{cases}$$ (1)

where $x = \varepsilon / \varepsilon_0$, $x = \sigma / \sigma_0$. More details about the definition of parameters have been fully documented by Han *et al*. (2005b).

Poisson's ratio (μ_c) in the elastic part of concrete under uniaxial compression stress ranges from 0.15 to 0.22, with a representative value of 0.19, according to ASCE (1982). In this numerical modeling, Poisson's ratio of concrete is taken as 0.19. The default values in ABAQUS (2003) are used for rest of the parameters: 55o for dilation angle, 0.667 for ratio of the second stress invariant on the tensile meridian to that on the compressive meridian, and 1.16 for ratio of initial equibiaxial compressive yield stress to initial uniaxial compressive yield stress.

2.2 Finite element model

When a concrete-filled column is subjected to an axial compressive load, the dominant deformation in the concrete core is compression without rotation, so a three-dimensional 8-node solid element (C3D8) would be the most effective element type to be used to reflect the concrete deformation characteristics. For steel tubes, both shell elements and solid elements were adopted in the previous research work (Han *et al*. 2005b, Dai and Lam 2010, Chang *et al*. 2012). In this paper, the three-dimensional eight-node isoperimetric solid element (C3D8) was also used for the steel tubes to ease the model set-up. This kind of element is a standard volume element of ABAQUS and more accurate if not distorted. Fig. 2 shows a schematic view of the element divisions for these two different CFTTS columns. A series of FE models with different element sizes were built to select the reasonable mesh that provides accurate results with lesser computational time. It was found that a mesh size of 20 mm is the appropriate one.

When a short concrete-filled steel column is compositely loaded, the concrete core and steel hollow section might experience different deformations; however, the bond action on their contacting surface will provide positive effects. Therefore, a surface-based interaction was used to represent the contact between the steel tube and the concrete. The friction between the two faces was maintained as long as the surfaces remained in contact. The hard contact between the concrete and the steel tube prevents the separation between the surfaces and, as a result, the interface becomes the boundary of the steel tube. Thus, both contact elements do not allow penetrating each other in the direction normal to the faces. And in the direction parallel to the interface, a coulomb law of friction is adopted and more detail about this model has been fully documented by ABAQUS User's Manual (2003). And the coefficient of friction between the two faces is 0.3 for
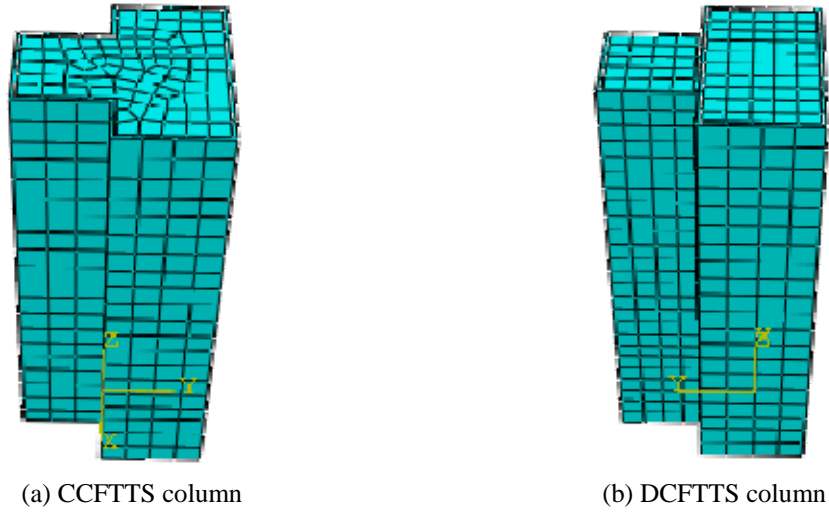
(a) CCFTTS column   (b) DCFTTS column

Fig. 2 Finite element mesh for CFTTS columns

Table 1 Geometrical parameters for all test specimens

Specimen ID	b_1/mm	b/mm	b_2/mm	h_1/mm	h_2/mm	t/mm	l/mm
C-1	50	100	50	100	100	2.9	450
C-2	50	100	50	100	100	3.8	450
C-3	50	100	50	100	100	4.6	450
C-4	60	80	60	100	100	3.8	450
C-5	35	80	35	100	100	3.8	450
C-6	25	150	25	100	100	3.8	450
D-1	35	80	35	100	100	4	450
D-2	60	80	60	100	100	4	450
D-3	25	150	25	100	100	4	450
D-4	50	100	50	100	100	3	450
D-5	50	100	50	100	100	4	450

all the FE models in this paper, which is discussed in the following section.

The top and bottom surfaces of the CFTTS columns were restrained against all degrees of freedom except the displacements at the loaded end in the direction of the applied load. The other nodes were free to translate and rotate in any direction. A uniform distributed load was applied statically at the top surface using the displacement control. The non-linear geometry parameter (NLGEOM) was excluded since only short columns are discussed in this paper.

2.3 Model validation

To validate the accuracy of the numerical model for CFTTS columns described in the previous section, nine previously published test specimens (Xu *et al*. 2009, Du *et al*. 2008) were used for

Table 2 Material parameters for steel tube in the test

Tube type	t / mm	E_s / GPa	f_y / MPa	f_u / MPa
100×200	3	192	314.57	411.21
100×100	3	188	306.17	392.65
100×100	4	200	291	419.53
100×150	4	190	315	427.75
100×80	4	190	270	355.25
100×100	5	193	300	381.42

comparison purpose. Table 1 summarizes the geometrical parameters for all the test specimens. In series "C", specimens are CCFTTS columns while specimens are DCFTTS columns in series "D". Table 2 gives the material parameters for steel tubes of the test DCFTTS specimens. For all the test specimens, the cube strength of concrete core (f_c) is 49.96 MPa.

Fig. 3 gives the comparison of computed load-longitudinal strain curves with the tested ones. It can be found that, generally good agreement is obtained between the predicted and tested results. This confirms that the present numerical model can be used with confidence to simulate the compressive behavior of the CFTTS columns.
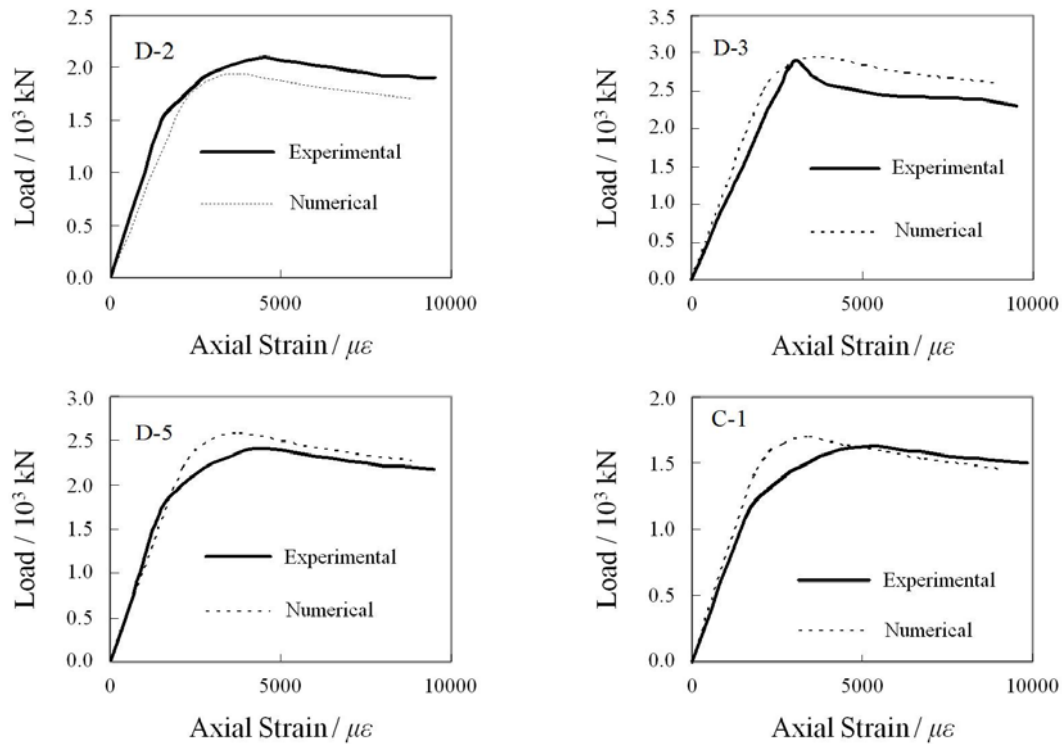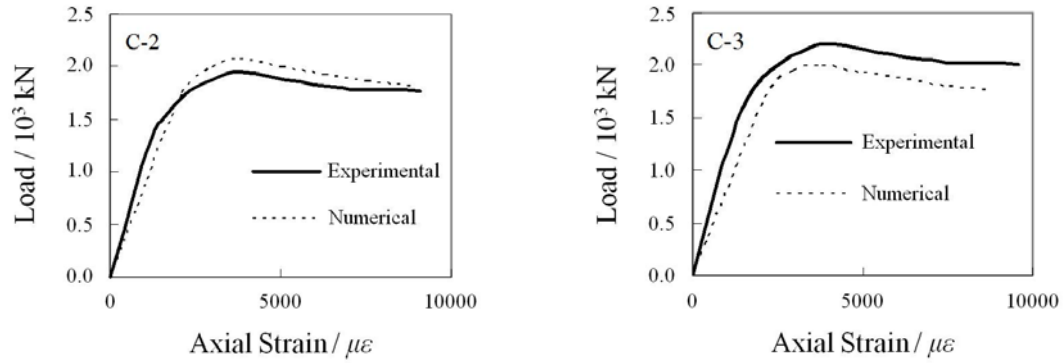

Fig. 3 Continued

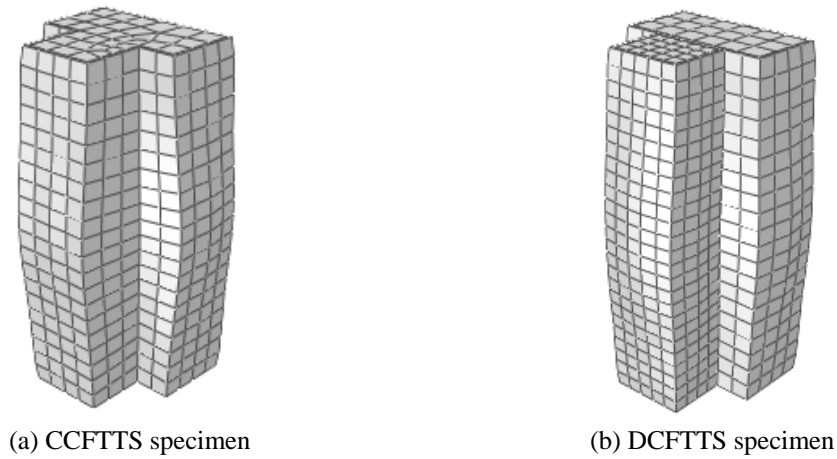Fig. 3 Comparison of numerical load-axial strain curves with experimental ones

(a) CCFTTS specimen   (b) DCFTTS specimen

Fig. 4 Typical failure mode of CFTTS specimens
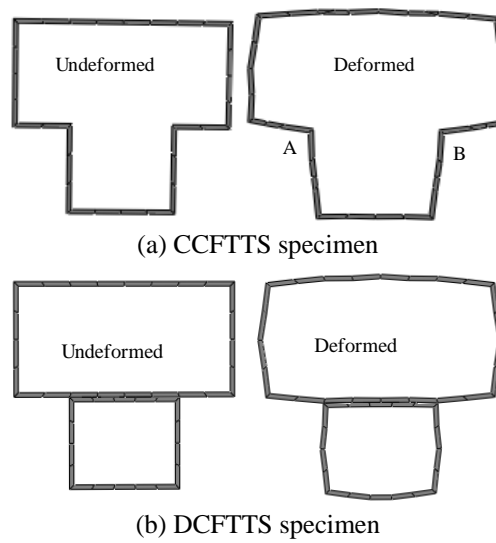

(a) CCFTTS specimen

(b) DCFTTS specimen

Fig. 5 Deformation of steel tubes for two types of CFTTS specimen

3. Analysis and discussion

3.1 Failure mode

Comparisons between the typical predicted failure modes of CCFTTS column and DCFTTS column are shown in Fig. 4. The calculating conditions are listed in Table 3 and both have the concrete cube strengths of 30MPa. Fig. 4 indicates both have the similar failure modes that the steel tubes are only outward buckling on all columns' faces because the presence of the concrete core prevents the occurrence of inward bucking. The deformation contour of steel tubes at middle section for CCFTTS column and DCFTTS column are compared in Fig. 5. From the above comparison, it could be found that the obvious deformation of the steel tubes for CCFTTS column occurs near the two corners (indicated as A and B in Fig. 5) that the included angles of the corners become more open. For DCFTTS column, dominated deformation occurs near the middle points of sides of the middle section.

In tests, the steel tube for DCFTTS column is welded by two individual tubes with rectangular/square cross section. Therefore, the DCFTTS column can be considered to consist of two common CFT columns. The failure modes of common CFT columns and their counterparts in DCFTTS column are compared in Fig. 6. It can be seen that the CFT columns outward bucking on four faces while their counterparts in the DCFTTS column only outward bucking on three faces duo to the interaction of these two parts.

3.2 Load-displacement curve

For better understanding of the axial loaded performance of the CFTTS columns, the typical load-displacement curves for the CCFTTS column and DCFTTS column are compared in Fig. 7. Both have the same geometrical and material parameters, as listed in Table 3. It is shown that both have the similar behavior that these curves can generally divided into three stages: the elastic stage (OA), elastic-plastic stage (AB) and plastic stage (rest of curve). During the elastic stage, there is no obvious difference between these two curves. However, the load of the CCFTTS column is becoming lower than that of the DCFTTS column after point A.

(a) Failure mode of two parts of DCFTTS specimen   (b) Failure mode of common CFT specimen
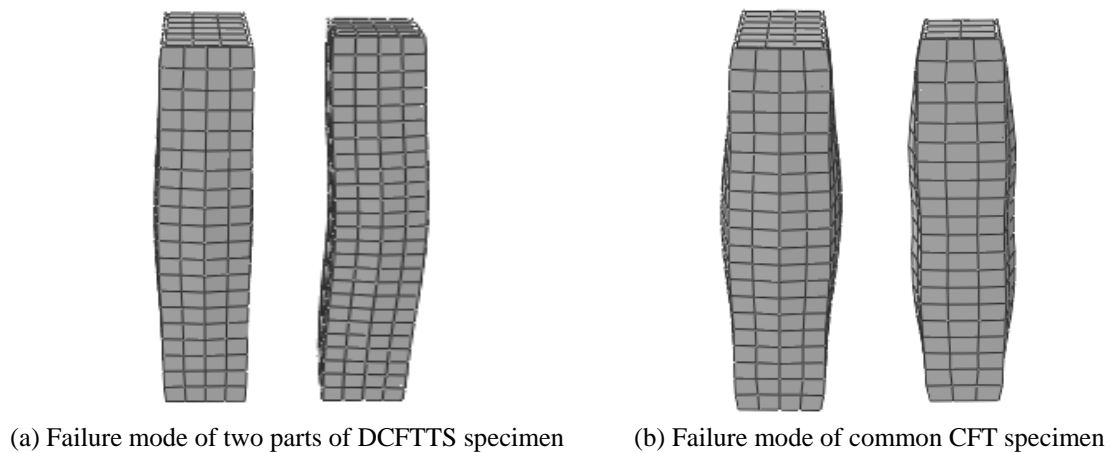
Fig. 6 The failure modes of common CFT columns and their duplicates in DCFTTS column
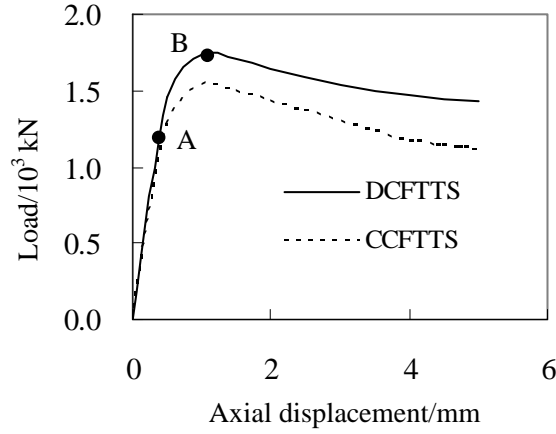
Fig. 7 Typical load-displacement curves for CCFTTS specimen and DCFTTS specimen

Table 3 Geometrical and material parameters for numerical model

Specimen type	b_1/mm	b/mm	b_2/mm	h_1/mm	h_2/mm	t/mm	f_y/MPa	f_u/MPa	E_s/GPa	v
DCFTTS	50	100	50	100	100	4	245	300	210	0.22
CCFTTS	50	100	50	100	100	4	245	300	210	0.22

As mentioned above, the DCFTTS column can be considered to consist of two common CFT columns. The load-displacement curves for the DCFTTS column and its parts, two common CFT columns are presented in Fig 8. For a given displacement, the sum of the loads for the two common CFT columns is approximately equal to the load of the DCFTTS column with an error of 0.2%. This indicates that, for the DCFTTS column, axial loaded performance can be described quantitatively by its parts, two common CFT columns.
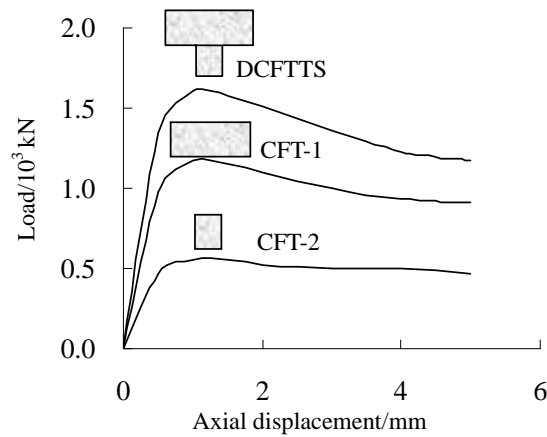

Fig. 8 Load-displacement curves for the DCFTTS column and its parts, CFT-1 and CFT-2

3.3 Confining effect

Fig. 9 shows the distributions of the longitudinal stress (S_{33} in the graphs) in the cross sections of the concrete core when the fiber of the outer steel tubes reaches yielding strength. It can be found from these figures that, generally, longitudinal stress in the concrete section is bigger near the corners of steel tube than the rest of the section. Also, it can be found that the confining effect for the CCFTTS columns is obviously less significant than that for the DCFTTS columns. When the fiber of the outer steel tubes reaches yielding strength, for the DCFTTS columns, only longitudinal stress in the central zone of concrete section is less than concrete strength (30 MPa). For the CCFTTS columns, only longitudinal stress near the corners is greater that concrete strength.

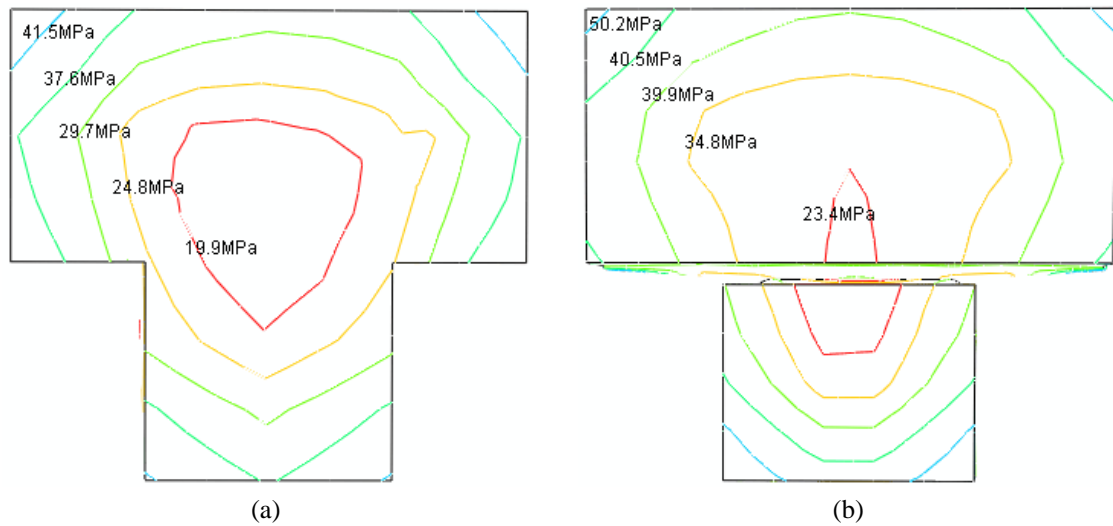(a)   (b)

Fig. 9 Longitudinal stress distributions: (a) cross section of concrete core for CCFTTS specimen; (b) cross section of concrete core for DCFTTS specimen
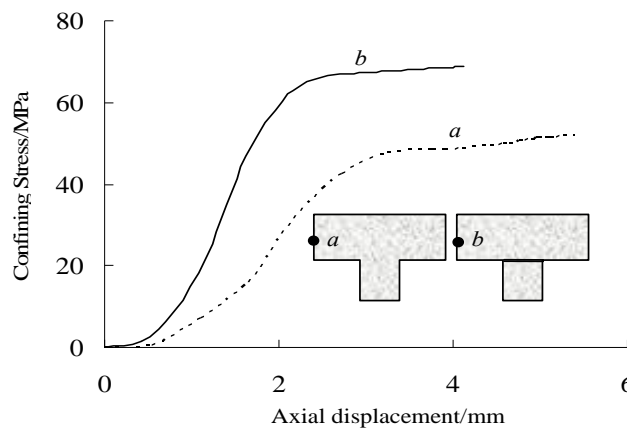

Fig. 10 Confining stress in the steel tube at two selected points

As a further effort to investigate the confining effect, the confining stress at two key points at middle height of the steel tubes for different columns are presented in Fig. 10. We can see that the confining stress increases continuously with increasing external load. The confining stress in the DCFTTS column is always higher than that in the CCFTTS column during the whole loading process. This can also contribute that, for the DCFTTS column, the steel tube can offer more sufficient confining effect on concrete core than that of the CCFTTS column. As a result, the DCFTTS column has higher axial loaded performances than CCFTTS column even with the same geometrical and material parameters (indicated in Fig. 7). It should be noted that the stress-strain relationship of the concrete core should be different for the two types of CFTTS columns because the confining effects by steel tube are different. However, no efforts have been made to set up a special stress-strain relationship for concrete core of the CFTTS columns in this paper since enough test data are currently unavailable. Further research efforts are need to develop a suitable stress-strain model for concrete core of the CFTTS columns to be used in FE analysis.

3.4 Parametric study

The possible parameters affecting axial capacity of the concrete-filled columns are thickness of steel tube (t) and concrete strength (f_{ck}). Hereinafter, the influences of the parameters mentioned above on are analyzed. All the data are the same as those listed in Table 3 if not specified.

3.4.1 Influence of tube thickness

In order to study the influence of tube thickness, we chose five different values of the tube thickness, t = 2, 4, 6, 8, 10 mm to setup models, while keeping other parameters constant. Fig. 11 presents the computed results that the axial capacities for both CCFTTS columns and DCFTTS ones increase with increasing tube thickness. However, the axial capacities for DCFTTS columns is always higher than that of the CCFTTS ones. The axial capacities for CCFTTS column and DCFTTS column are 1228 and 1330 kN when the tube thickness is 2.0 mm. When the tube thickness increases to 8 mm the axial capacities for CCFTTS column and DCFTTS column are 2320 and 2700 kN, respectively. The differences of axial capacities are 102 kN and 380 kN,
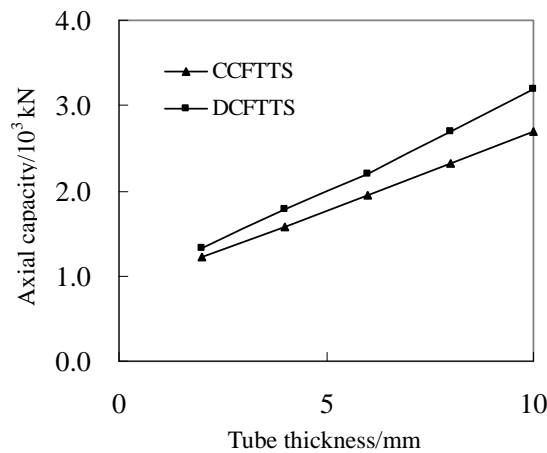

Fig. 11 Axial capacities for CFTTS column

respectively. It indicates that the differences of axial capacities increase with increasing tube thickness. This contributes that, for DCFTTS columns, the steel tube can give more "significant" utilization to axial capacity with higher tube thickness.

3.4.2 Influence of concrete strength

Fig. 12 gives the influence of concrete strength on axial capacities. It can be seen that increasing the strength of the concrete core, for both CCFTTS columns and c DCFTTS columns, leads, to a linear increase in the columns strength, at least for the range of concrete strengths investigated herein (20-60 MPa).

3.4.3 Influence of friction coefficient between steel tube and concrete core

As mentioned above, friction coefficient might provide positive effect on axial performance of CFTTS columns. However, selection of the friction coefficient is difficult because there is no
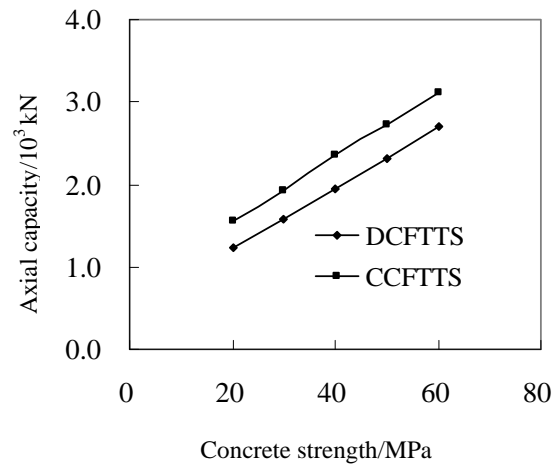

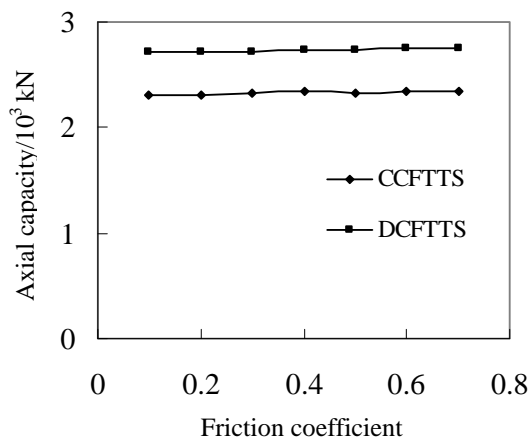Fig. 12 Influence of concrete strength on axial capacity

Fig. 13 Influence of friction coefficient on axial capacity

standard test procedure to determine it. Therefore, in this section, different friction coefficients, from 0.1 to 0.7, was selected to explore their effect on column strength. Other parameters are the same as those listed in Table 3. Fig. 13 gives the computed results that there was little effect on the axial resistance when different friction coefficients were used. A convergent problem is induced when the friction coefficient is greater than 0.8. Therefore a friction coefficient of 0.3 is suggested to achieve a quick convergence.

4. Calculation of axial capacity

4.1 Axial capacity of DCFTTS column

According to the analysis mentioned above, a DCFTTS column can be considered to consist of two common CFT columns. Therefore, axial of the DCFTTS column could be considered the sum of the strength of two common CFT columns

$$P_c = P_1 + P_2 \tag{2}$$

where, P_c is strength of DCFTTS column. P_1 and P_2 are the strength of the common CFT column, which can be calculated according to the existing design specifications.

To verify the validity of the proposed design model, five tested specimens have been considered. The main parameters of these tests are listed in Tables 1 and 2. The experimental axial capacities compared with those calculated by Eq. (2) with ACI design specifications are presented in Fig. 14.

4.2 Axial capacity of common CCFTTS column

We can contribute that, for common CCFTTS column, steel tube provides smaller confining effect on the concrete core. The axial capacity is mainly determined by the contributions of concrete and steel tube. So, the strength for common CCFTTS column can be calculated by
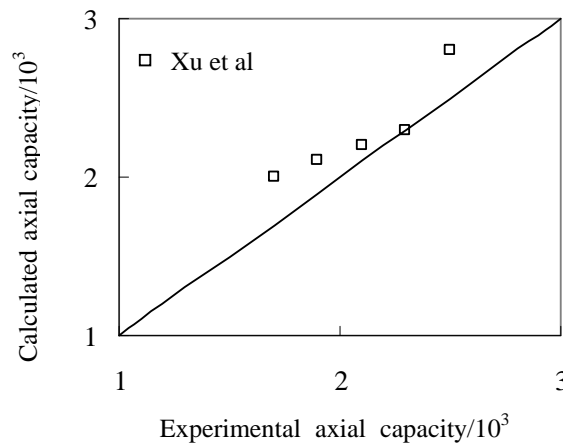

Fig. 14 Comparison of axial capacity between Eq. (2) and test results
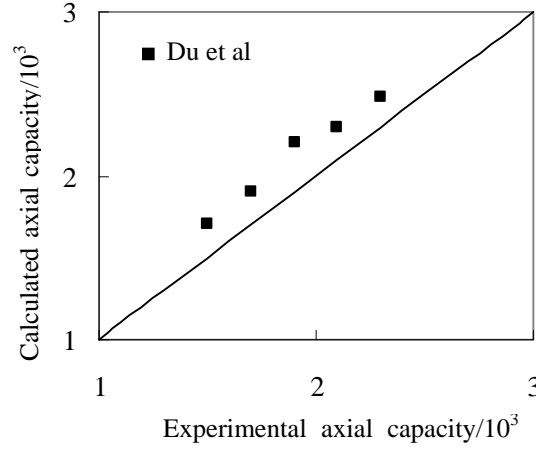
Fig. 15 Comparison of axial capacity between Eq. (2) and test results

$$P = A_c f_{ck} + A_s f_y \qquad (3)$$

where f_{ck} is taken as $0.76 f_c$.

The calculated results according to Eq. (3) for all the tested specimens are presented in Fig. 15. Generally, the calculated column strength is lower than tested one, with an error of less than 7%. This is because that, in Eq. (3), the confining effect on the concrete core offered by the steel tube is neglected. This assumption leads to an underestimation of the strength of the column; however, it is acceptable since corresponding predictions are on the safe side. Also, Eq. (3) is simple and convenient in design.

5. Conclusions

The compressive behaviors of concrete-filled steel tube columns with "T" shaped cross section are investigated through the ABAQUS/Standard solver. The mechanisms of columns with two types of "T" shaped cross section (CCFTTS column and DCFTTS column) are discussed. The feasibility and accuracy of the numerical method was verified by comparing the calculated results with the experimental observations, and the following conclusions are made within the limitations of the research work in this paper.

- For both CCFTTS column and DCFTTS one, the failure modes is that the steel tubes are only outward buckling on all columns' faces.
- For DCFTTS column, the steel tube can offer more significant confining effect on concrete core than that of CCFTTS column. Therefore, the DCFTTS column has higher axial capacity than CCFTTS column even with the same geometrical and material parameters.
- A parametric study is also conducted to analyze the effects of tube thickness, concrete strength and friction coefficient on axial capacities of CFTTS column.
- A simplified model is developed for calculating the axial capacities of two types of CFTTS columns. Comparisons are made between the calculated axial capacities and the tested results.

It was found that the calculated axial capacities are in general agreement with those of the testing.

Acknowledgements

References

ACI 318-95 (1999), *Building code requirements for structural concrete and commentary*, American Concrete Institute, Detroit, MI, USA.

ASCE (1982), *ASCE task committee on concrete and masonry structure*, New York, State of the Art Report on Finite Element Analysis of Reinforced Concrete.

Chang, X., Wei, Y.Y. and Yun, Y.C. (2012), "Analysis of steel-reinforced concrete-filled steel tubular (SRCFST) columns under cyclic loading", *Constr. Build. Mater.*, **28**(1), 88-95.

Dai, X. and Lam, D. (2010), "Numerical modeling of the axial compressive behaviour of short concrete-filled elliptical steel columns", *J. Constr. Steel. Res.*, **66**(7), 1057-1069.

Du, G.F., Xu, L.H., Weng, F. and Xu, H.R. (2008), "Test study on behavior of T-shaped concrete filled steel tubular short columns under axial compression", *J. HUST (Urban science edition)*, **25**(3), 188-194. [in Chinese].

Ellobody, E., Young, B. and Lam, D. (2006), "Behaviour of normal and high strength concrete-filled compact steel tube circular stub columns", *J. Constr. Steel. Res.*, **62**(7), 113-134.

Han, L.H. (2007), *Concrete-Filled Steel Tubular Structures*, *Theory and Practice*, Science Press, Beijing, China. [in Chinese].

Han, L.H., Yao, G.H. and Zhao, X.L. (2005a), "Tests and calculations of hollow structural steel (HSS) stub columns filled with self-consolidating concrete (SCC)", *J. Constr. Steel. Res.*, **69**(1), 1241-1269.

Han, L.H., Yao, G.H., Chen, Z.P. and Yu, Q. (2005b), "Experimental behaviour of steel tube confined concrete (STCC) columns", *Steel Compos. Struct.*, *Int. J.*, **5**(6), 459-484.

Hibbitt, Karlson & Sorensen Inc. (2003), *ABAQUS/standard User's Manual*, Version 6.4.1., Pawtucket, RI, USA.

Hu, H.T. and Schnobrich, W.C. (1989), "Constitutive modeling of concrete by using non-associated plasticity", *J. Mater. Civ. Eng.*, **1**(4), 199-216.

Hu, H.T., Huang, C.S., Wu, M.H. and Wu, Y.M. (2003) "Nonlinear analysis of axially loaded concrete-filled tube columns with confinement effect", *J. Struct. Eng.*, *ASCE*, **129**(10), 1322-1329.

Mander, J.B., Priestley, M.J.N. and Park, R. (1988), "Theoretical stress-strain model for confined concrete", *J. Struct. Eng.*, *ASCE*, **114**(8), 1804-1826.

Nardin, S. and Debs, E.l. (2007), "Shear transfer mechanisms in composite columns: an experimental study", *Steel Compos. Struct.*, *Int. J.*, **7**(5), 377-390.

Saenz, L.P. (1964), "Discussion of the paper: Equation for the stress-strain curve of concrete (by P. Desayi, and S. Krishnan)", *J. Am. Concrete Inst.*, **61**, 1229-1235.

Shanmugam, N.E. and Lakshmi, B. (2001), "State of the art report on steel-concrete composite columns", *J. Constr. Steel Res.*, **57**(10), 1041-1080.

Tao, Z., Uy, B., Han, L.H. and Wang, Z.B. (2009) "Analysis and design of concrete-filled stiffened thin-walled steel tubular columns under axial compression", *Thin-Wall. Struct.*, **47**(12), 1544-1556.

Uenaka, K., Kitoh, H. and Sonoda, K. (2008), "Concrete filled double skin tubular members subjected to bending", *Steel Compos. Struct.*, *Int. J.*, **8**(4), 297-312.

Uy, B. (2001), "Strength of short concrete filled high strength steel box columns", *J. Constr. Steel Res.*, **57**(1), 113-134.

Xu, L.H., Du, G.F., Weng, F. and Xu, H.R. (2009), "Experimental study on normal section compression bearing capacity of composite "T" shaped concrete filled steel tubular columns", *China Civ. Eng. J.*, **42**(6), 14-21. [in Chinese].

CC